

**DIFFERENT REGIMES OF STRIPE FLUCTUATIONS  
IN THE SUPERCONDUCTING CUPRATES**

*G.V. Teitel'baum*

Institute for Technical Physics of the RAS, 420029 Kazan, Russia

**РАЗЛИЧНЫЕ РЕЖИМЫ ФЛУКТУАЦИЙ  
В ФАЗОВОМ РАССЛОЕНИИ СВЕРХПРОВОДЯЩИХ КУПРАТОВ**

*Г.В. Тейтельбаум*

Физико-технический институт РАН, Казань



*Volume 6, No. 1,  
pages 221-228, 2004*

<http://mrsej.ksu.ru>

**DIFFERENT REGIMES OF STRIPE FLUCTUATIONS  
IN THE SUPERCONDUCTING CUPRATES**

G.B. Teitel'baum

*Institute for Technical Physics of the RAS, 420029 Kazan, Russia*

The complementary NMR and ESR studies of the frustrated phase separation in different superconducting cuprates are reported. We specially address the temperature dependence of the magnetic fluctuations and discuss their link with the observed superconducting state. It is argued that according to the phase diagram obtained for the lanthanum cuprates the superconducting phase coexists with the developed antiferromagnetic correlations. The observed picture is strongly dependent on the hole doping. In the vicinity of 1/8 doping such a coexistence may be realized in a form of dynamic stripes – the corresponding enhancement of the spin-stiffness reveals the plane character of the spin (and charge) inhomogeneities. Depending on whether these inhomogeneities are pinned or not, one has to distinguish the static and dynamical regimes of stripe fluctuations. With a help of our spin stiffness estimations, the upper threshold values of this quantity critical for the superconducting state were determined. The NMR analysis of the stripe phase local properties made it possible to estimate the local magnetic moment corresponding to antiferromagnetic domains as well as the charge of the domain walls.

## I. Introduction

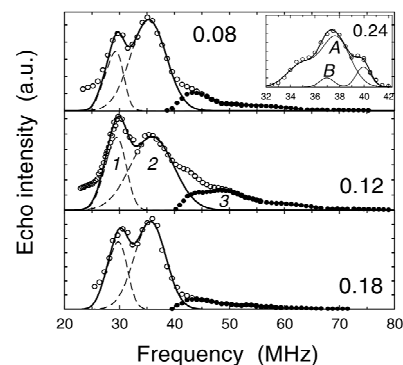
Soon after the discovery of high- $T_c$  superconductivity in cuprates by Bednorz and Müller it was found that these materials reveal the intrinsic tendency to the phase separation [1]. One of the possible manifestations of this feature upon doping of the parent antiferromagnetic (AF) phase of a high- $T_c$  superconductor by holes is the segregation of charges to the periodical domain walls (stripes) separating the antiphase AF domains [2,3]. The first evidence for such stripe phase has been provided by neutron studies of the low temperature tetragonal (LTT) phase of Nd-doped  $\text{La}_{2-x}\text{Sr}_x\text{CuO}_4$  [3]. Later the stripe correlations were observed in other cuprates [4-6]. But in spite of the hot interest to the problem, surprisingly little is known about the local properties of the stripe structure as well as about their relevance to the origin of the high- $T_c$  mechanism. One of the key problems here is the elucidation of the possible coexistence of stripe fluctuations with the superconductivity. Investigations of this problem with different experimental methods give evidence that the observed picture is highly dependent on the characteristic frequency scale of the method. This indicates that relationship of the superconductivity and the stripe fluctuations is strongly frequency dependent.

In the present paper we overview the complementary NMR and ESR studies of different frequency regimes of the stripe fluctuations in the lanthanum cuprates. The essential feature of our approach is that it is connected with the tuning of the fluctuation's frequencies of the studied materials by various doping. The possibility of such a tuning is related with the different ways to affect the structure: *i*) the strontium doping reduces the magnitude of the  $\text{CuO}_6$  octahedra tilts and may induce the transition between the LTO (Low Temperature Orthorhombic) and HTT (High Temperature Tetragonal) phases; *ii*) the doping by the rare earth ions controls the direction of the  $\text{CuO}_6$  octahedra tilts and may induce the transition between the LTO and LTT (Low Temperature Tetragonal). The different octahedra tilts result in different buckling of  $\text{CuO}_2$  planes thus providing the different pinning of the stripe fluctuations.

## II. The stripes fluctuations in LTT phase

1. This part of the paper is devoted to the NQR studies of cuprates with LTT structure, which is helpful for pinning of the stripe phase. This structure was induced by doping with non-magnetic Eu rare-earth ions instead of magnetic Nd ones used in [3] (the ordering of Nd moments causes fast Cu nuclear relaxation hindering the observation of Cu NQR). We expect that in the stripe structure the different Cu sites will be inequivalent with respect to the NQR, providing information on the local properties at given points of the structure. The serious difficulties of the present research are due to the slowing of the charge fluctuations down to MHz frequency range which wipes out a large part of the nuclei from the resonance [7,8]. Fortunately the reappearance of the signal in the slow fluctuations limit at low temperatures enables us [9] to take the advantages of the extreme sensitivity of Cu NQR to the local charge and magnetic field distribution.

Fig. 1. Representative Cu NQR lineshapes at 1.3 K of  $\text{La}_{2-x}\text{Eu}_y\text{Sr}_x\text{CuO}_4$  with  $y = 0.17$ . The value of  $x$  is shown for each line. All lineshapes include standard frequency corrections of  $v^2$  and are normalized to equal heights. The continuous line is the fit of the two-isotope contribution of sites 1 and 2. Filled circles show the contribution of the antiferromagnetic site 3. Inset: A typical signal for  $x > 0.18$  decomposed into two contributions ( $T = 4.2$  K)



2. For our experiments we have chosen fine powders  $\text{La}_{2-x}\text{Eu}_y\text{Sr}_x\text{CuO}_4$  with variable Sr content  $x$  and fixed Eu content  $y = 0.17$ . The preparation of single-phase samples was described in [10]. It was found [10] that for such Eu content the LTT phase is realized for  $x > 0.07$ . For Sr concentrations  $x > 0.12$  the ac-susceptibility and microwave absorption measurements reveal the presence of superconductivity with  $T_c = 6; 9; 14; 19; 18; 16; 13\text{K}$  for respectively  $x = 0.12; 0.13; 0.15; 0.18; 0.20; 0.22; 0.24$ . The superconducting fraction is small for  $x \leq 0.18$  and starting from  $x > 0.18$  a transition to bulk superconductivity takes place.

The NQR measurements were performed with the standard spectrometer in the range 20 - 100 MHz. By lowering the temperature down to 1.3 K, the Cu-NQR spectra at all Sr concentrations were observed [9].

Regarding their NQR properties the samples should be separated into two groups:

The first one corresponds to Sr concentrations  $x \leq 0.18$ . The superconducting fraction of these samples, if any, was rather small. Each of the spectra, which are very similar for  $0.08 \leq x \leq 0.18$ , consists of a broad line in the region from 20 MHz up to 80 MHz with an unresolved peak between 30 and 40 MHz (Fig. 1). The spectra for different  $x$  differ mainly with the integral intensity, which is peaked near  $x = 0.12$  (Fig. 2a).

The second group of samples with  $x > 0.18$  showing bulk superconductivity possesses completely different and much narrower NQR spectra (Inset to Fig. 1), which can also be observed at much higher temperatures. The intensity grows up with increasing  $x$  from 0.18 (Fig. 2b).

3. Beginning the discussion with the  $x \leq 0.18$  group, let us first consider the above-mentioned complicated peak in the lineshapes. The two Cu-isotopes Gaussian fit to these peaks reveals the existence of two independent copper sites 1 and 2 having different NQR frequencies (Fig. 3).

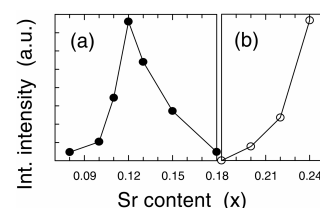


Fig. 2. The Cu NQR integrated intensity (normalized) of  $\text{La}_{2-x}\text{Eu}_y\text{Sr}_x\text{CuO}_4$ : for  $0.08 \leq x \leq 0.18$  at 1.3 K (a); for  $x \geq 0.18$  at 4.2 K (b)

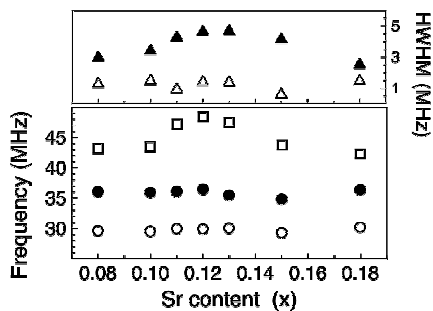


Fig. 3 The parameters of different contributions to the Cu NQR signal for  $0.08 \leq x \leq 0.18$  in  $\text{La}_{2-x}\text{Eu}_x\text{CuO}_4$  ( $T = 1.3$  K):  $^{63}\text{Cu}$  NQR frequencies of sites 1 - open circles and 2 - filled circles; the corresponding half widths at half maximum (HWHM) - open and filled triangles resp.; the frequencies corresponding to the maxima of the magnetic contribution 3 are shown by squares

via the relation  $\nu_Q(n, H) = \nu_Q^0(H) + \beta n$  with the empirical constant  $\beta$  and  $H(\mathbf{r})$  being the internal magnetic field. The first term here is the NQR frequency for the compound with zero Sr content, the second one is the positive shift due to the local increase of the effective fractional charge on Cu. This expression agrees both with the calculations in the ionic [11] as well as in the cluster [12] models (in the uniform case  $n = x$ ).

It follows from our results (Fig. 3) that the resonance frequencies  $^{63}\nu_Q^{(1)}(x)$  for line 1 are shifted to lower values from the reference value  $^{63}\nu_Q(0,0) = ^{63}\nu_Q^0$  (we use here  $^{63}\nu_Q^0 = 31.9$  MHz estimated for  $\text{La}_2\text{CuO}_4$  [13]). This indicates that the positive contribution to  $^{63}\nu_Q(x,n)$  is small and that the effective fractional charge on sites 1 is near zero. The corresponding resonance frequency depends on the local internal field and has a minima for Zeeman frequencies falling in the vicinity of bare quadrupole frequency  $^{63}\nu_Q^0$ . The distribution of the resonance frequencies is enhanced at the point corresponding to the minima giving rise to a narrow line 1. In contrast, line 2 is due to the sites which exhibit a positive shift respect to  $^{63}\nu_Q^0$ . It means that these sites belong to the regions with an increased average charge (hole density) on the Cu ions. The high frequency part of the spectrum can be analyzed by subtraction of the 1 and 2 contributions from the entire signal. The resulting spectra are shown in Fig. 1. The frequencies corresponding to their maxima are plotted in Fig. 3. We assume that this line corresponds to the broadened  $1/2 \leftrightarrow -1/2$  transitions of nuclei located in sites 3 experiencing an internal magnetic field (note the broad high-frequency shoulder). The satellites are unresolved due to inhomogeneities of the internal magnetic field and of the NQR frequencies. If the orientation of the internal field with respect to the electric field gradient is identical to that observed for  $\text{La}_2\text{CuO}_4$  [13] the frequency of this transition enables us to estimate the quadrupole shift and to determine the Larmor frequency for this Cu site to be 45.2 MHz for  $x = 0.12$ . It corresponds to an internal field of 40.1 kOe. Using the hyperfine constant  $|A_Q| = 139$  kOe/ $\mu_B$  [14], we estimate the effective magnetic moment of Cu at site 3 to be equal to  $0.29 \mu_B$ , coinciding with the value obtained from neutron and muon experiments [4,15].

Since quantitatively similar spectra were observed for each compound of the first group we believe that they contain the same elementary "bricks" of the phase under study. Discussing the relative weight of the different contributions and extrapolating the corresponding signal intensities to  $t = 0$  we find the contributions of sites 1, 2, 3 to be given by the ratio (1:6:13).

For the interpretation of our results it is important that signal 1 is not connected with any specific feature of the structure, whereas the signals 2 and 3 correspond to the extremal points of the spin and charge distributions.

The NQR frequencies for the site 2 (see Fig. 4) are almost the same for any  $x$  thus indicating that for all Sr concentrations the stripes are equally charged. The effective charge in a stripe is near 0.18 - 0.19. This is larger than the average hole concentration ( $x$ ) but less than 0.5 expected for the ideal stripe picture [3]. It means that the charge is distributed over the domain wall of a finite thickness. Together with the above-mentioned intensity ratio this indicates that the real stripe picture differs from the ideal one. The changes in intensity of the NQR spectra are due to variation of the number of "bricks" for the compounds with different  $x$ , which depends on the pinning strength. Our results indicate that the stripe phase is pinned at least for the time scales shorter than  $10^{-6}$  sec (so called quasistatic regime).

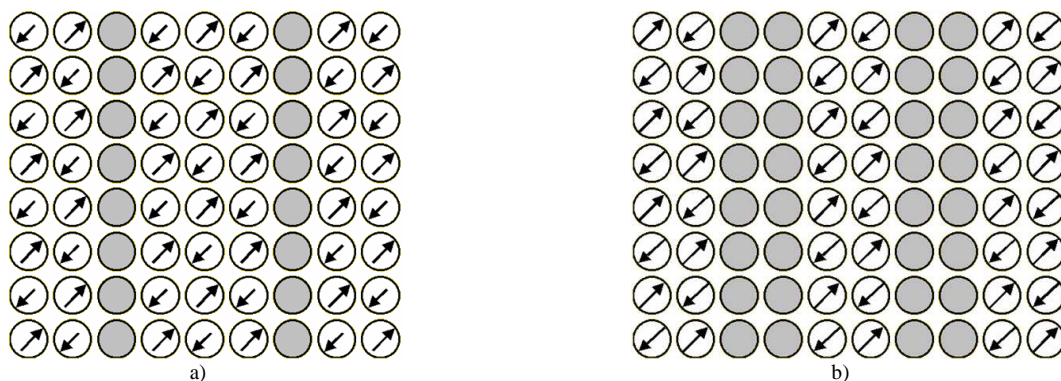


Fig. 4. The possible models of the stripe structure: **a)** charged ( $n = 0.5$ ) stripes and three-leg spin ladders; **b)** charged ( $n = 0.25$ ) stripes and two-leg spin ladders. The circles represent the copper ions whereas the arrows indicate the magnetic moment's orientation. The shadowed circles correspond to the nonmagnetic sites with the distributed hole density

The pinning for  $0.08 \leq x \leq 0.18$  is due to the buckling of the  $\text{CuO}_2$  plane. It is connected with the  $\text{CuO}_6$  octahedra tilts around the [100] and [010] axis by the angle  $\Phi$ , which for given Eu substitution is governed by the Sr content. It follows from Fig. 2a, that the quantity of the pinned phase, which is proportional to the NQR signal intensity, is peaked at  $x = 0.12$  when according to our estimations the entire sample is in the pinned stripe phase. This indicates additional strong pinning due to the commensurability effect. Such pinning is not unique for the LTT phase (as buckling is). It is a manifestation of the plane character of the inhomogeneities of the charge and spin distributions. Together with the existence of three different Cu sites (note that site 1 corresponds to a defect) this gives an independent justification of the stripe picture. Our data are compatible with two models: *i*) the structure [3] with the charge domain wall along one Cu-O chain separated by the bare three-leg ladders (Fig. 4a). The deviation of the estimated effective charge from 0.5 may indicate that in reality the thickness of the charged stripe is larger than one lattice spacing; *ii*) the structure [16] with the charged walls consisting from two neighboring Cu-O chains separated by two-leg spin ladders (Fig. 4b). The average hole density in this model is 0.25. This is closer to the observed 0.19, but there are some problems with the relative intensity of the sites 2 and 3 and the periods of spin and charge modulations.

Upon increasing  $x$  over  $x = 0.18$  the tilt angle is decreasing below the critical value  $\Phi_c \cong 3.6^\circ$  [17] and depinning of the stripe phase takes place (i.e. transition to the dynamical regime). Such behaviour occurs for the compounds with Sr concentration  $x > 0.18$ . The corresponding NQR spectrum transforms to the narrow signal at higher frequencies, which for  $x = 0.24$  is shown in the inset to Fig. 1. The intensity of this line (proportional to the quantity of the unpinned stripe phase) is shown in Fig. 2b.

The analysis of this relatively narrow signal reveals only two different sites with  $^{63}\text{Cu}$  NQR frequencies of 37.60 MHz and 39.82 MHz. Within 1% accuracy these frequencies coincide with those known at the same  $x$  for the *A* and *B* sites in the LTO superconducting phase [18] confirming that the LTT structure differs only in the directions of  $\text{CuO}_6$  octahedra tilts. The satellite *B* is due to Cu having a localized hole in the nearest surrounding since, according to [12, 19], its NQR frequency has the additional positive shift  $\delta\nu_0 \cong 2.5$  MHz. The observed transformation of the NQR spectra in comparison with those for  $x \leq 0.18$  is due to the fast transverse motion of stripes in the depinned phase. As a result the internal magnetic field on Cu nuclei is averaged out, and the effective fractional charge is homogeneously distributed over all Cu nuclei giving usual NQR frequencies. A transition from the quasistatic to the dynamical regime of fluctuations, which is due to depinning, leads to drastic changes in the magnetic and superconducting properties.

Regarding the superconducting properties we note that the depinning point separates two different types of superconductivity. For  $x \leq 0.18$  we are dealing with a weak Meissner effect, an increased London penetration length and with  $T_c$  increasing with  $x$  growing up to 0.18. Combining these facts with the absence of a narrow signal typical for the bulk superconducting phase, indicating that the impure LTO phase is absent, and with the suppression of the relaxation via magnetic moments of doped holes, one has arguments in favor of possible one-dimensional superconductivity along the charged rivers of stripes – the issue which is widely discussed [20]. For  $x > 0.18$  we have bulk superconductivity with conventional London length, typical NQR signal and decreasing  $T_c(x)$ . Such crossover may be caused by the transverse motion of the stripes carrying superconducting currents, which gives rise to the conventional superconductivity in  $\text{CuO}_2$  planes. Although possibly a simple coincidence, it happens when the doping  $x$  is equal to the effective charge ( $n$ ) in a stripe.

### III. The stripe fluctuations in the LTO phase

1. The interest to the microscopic phase separation in the superconducting  $\text{La}_{2-x}\text{Sr}_x\text{CuO}_4$  has received a new impetus after the recent neutron scattering experiments [21,22] in the LTO phase of  $\text{La}_{2-x}\text{Sr}_x\text{CuO}_4$  with moderate  $x$  which reveal the presence of modulated AF order very similar to that observed in the LTT compound  $\text{La}_{1.6-x}\text{Nd}_{0.4}\text{Sr}_x\text{CuO}_4$ . But on a larger time scale magnetic fluctuations in  $\text{La}_{2-x}\text{Sr}_x\text{CuO}_4$  are dynamical, especially for the superconducting state, and their relevance to the stripe structure is a matter of debate. In particular, the dynamical nature of the microscopic phase separation hinders the investigation of its properties by means of low frequency local methods such as conventional NMR.

Therefore it is of great importance to investigate the phase diagram and the properties of magnetic fluctuations in superconducting  $\text{La}_{2-x}\text{Sr}_x\text{CuO}_4$  and related compounds shifting the measurements to larger frequencies. This section is devoted to analysis of the  $\text{Gd}^{3+}$  EPR measurements [23,24] which are focused mainly on the investigation of the temperature and doping dependence of the low frequency magnetic fluctuations for the superconducting  $\text{La}_{2-x}\text{Sr}_x\text{CuO}_4$  with hole doping covering the entire superconducting region of the phase diagram.

The temperature behaviour of the multiline  $\text{Gd}^{3+}$  ESR spectrum for  $T > T_c$  is qualitatively very similar to that observed for the Eu doped  $\text{La}_{2-x}\text{Sr}_x\text{CuO}_4$  compounds (with LTT symmetry) described in [24,25]: a linear dependence of  $\Delta H$  on temperature which is followed by the rapid growth of the linewidth at low  $T$  (the typical temperature dependence of the  $\Delta H$  for the most intense central component is shown in Fig. 5). But after cooling below 40 K the behaviour of superconducting and nonsuperconducting (Eu doped) samples becomes different: the linewidth of superconducting LSCO exhibits the downturn starting at a temperature  $T_m$ , dependent on  $x$ , whereas for other samples which are not bulk superconductors  $\Delta H$  continues to grow upon further lowering temperature (see Fig. 5).

2. We address now the question – why the temperature dependences for

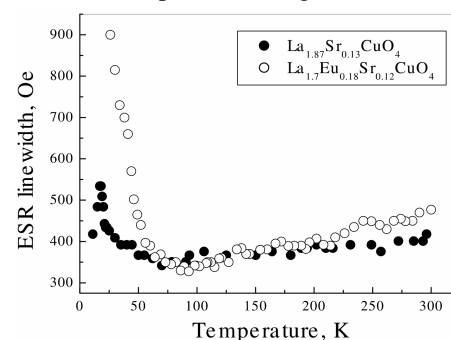


Fig. 5. The  $\text{Gd}^{3+}$  ESR linewidth temperature dependence for LTO superconducting LSCO and LTT nonsuperconducting LESCO

the nonsuperconducting (LTT) and superconducting (LTO) compounds are so different at low temperatures? To find an answer we take into account that in addition to the important but temperature independent residual inhomogeneous broadening the linewidth is given by different homogeneous contributions linked to the magnetic properties of the CuO<sub>2</sub> planes:

I) the interaction of Gd<sup>3+</sup> spins with the charge carriers, i.e. the Korringa relaxation channel. The simplest Korringa term in the linewidth is  $\Delta H = a + bT$  with  $b = 4\pi(JN_F)^2 P_m$  [26], where  $P_m = [s(s + 1) - m(m + 1)]$  – is the squared matrix element of the Gd spin-state transitions,  $N_F$  is the density of states at the Fermi level,  $J$  is the coupling constant between the Gd and charge carrier spins. For the system under study it was discussed in [27]. Note, that the enhancement of the linear slope for the Eu doped compound is due to the influence of the depopulation of the first excited magnetic Eu level [25].

II) the interaction of Gd with the AF fluctuations of copper spins, giving rise to the homogeneous broadening of the Gd ESR line (a close analogue of the nuclear spin-lattice relaxation). Introducing the internal field at Gd site,  $H_{Gd}$ , and averaging over the random orientation of the local Cu moments with respect to the external magnetic field it is possible to write the corresponding contribution to the linewidth as

$$\Delta H = \frac{1}{3}(\gamma H_{Gd})^2 P_m \left[ \tau + \frac{2\tau}{1 + (\omega_s \tau)^2} \right]. \quad (1)$$

Here  $\tau = \tau_\infty \exp(E_a/kT)$  is the life-time of AF fluctuations,  $\tau_\infty$  is its value at the infinite temperature, and  $E_a$  is the activation energy, proportional to the spin stiffness  $\rho_s$  ( $E_a = 2\pi\rho_s$ ),  $\omega_s$  is the ESR frequency.

This term describes the standard Bloembergen-Purcell-Pound (BPP) behaviour: the broadening of the EPR line upon cooling with the downturn at a certain freezing temperature  $T_m$  corresponding to  $\omega_s \tau = 1$ . It was observed in [23,24,27] that depending on the Sr content the linewidth behaviour transforms from the BPP-like (with the maximum at  $T_m$ ) to the pure Korringa (linear) temperature dependence. Based on the observation that the relative weight of the BPP-contribution compared with the Korringa one decreases with increasing Sr doping, it was concluded [23,24] that at low  $x$  the Gd spin probes the almost magnetically correlated state and at the high  $x$  – the almost nonmagnetic metal. The corresponding phase diagram is shown in Fig. 6.

The different temperature dependences of the superconducting and nonsuperconducting samples may be explained assuming that for the superconducting samples the linewidth below  $T_c$  is governed by fluctuating fields which are transversal to the magnetic field responsible for the Zeeman splitting of the Gd spin states (the second term in Eq.(1)). Since these fluctuations are induced by Cu moments lying in the CuO<sub>2</sub> planes, it means that Gd ions are subjected to the constant magnetic field normal to these planes. This may indicate that the magnetic flux lines penetrating in the layered superconducting sample tend to orient normally to the basal planes where the circulating superconducting currents flow. (The difference of the  $T_m$  and  $T_c$  values observed for the samples with small  $x$  enables one to conclude that the possible distortion of ESR lineshape owing to the non-resonant microwave absorption as the main reason for the apparent narrowing of the ESR line below  $T_c$  seems to be improbable).

Since the measurements [23,24] were carried out at nonzero external field it is very important to consider the flux lattice effects. At typical ESR fields of  $\sim 0.3$  T, which are oriented normal to the CuO<sub>2</sub> layers, the period of the lattice is 860 Å, whereas the vortex core sizes for La<sub>2-x</sub>Sr<sub>x</sub>CuO<sub>4</sub> is 20 Å. As the upper critical field equals to 62 T, it is clear that in the case of ESR the vortex cores occupy only 0.5% of the CuO<sub>2</sub> planes. According to [28,29] the Cu spins in the vortex cores may be AF ordered. Therefore the phase diagram in Fig. 6 indicates that not only the spins in the normal vortex cores are AF correlated, but the AF correlations are spread over the distances of the order of magnetic correlation length which at low doping reaches 600 - 700 Å [29].

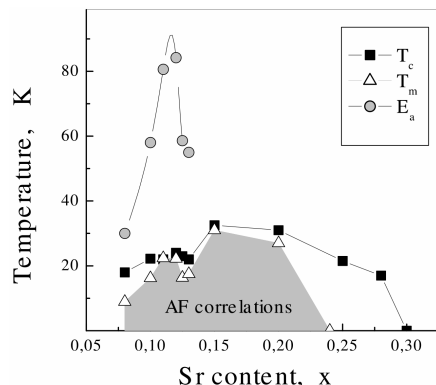


Fig. 6. The fluctuation's phase diagram of the superconducting La<sub>2-x</sub>Sr<sub>x</sub>CuO<sub>4</sub>. The triangles correspond to the magnetic transition temperature  $T_m(x)$ , squares – to the superconducting transition temperature  $T_c(x)$  and the circles to the magnetic fluctuations activation energy  $E_a(x)$

3. Numerical simulations of the temperature dependences of the Gd ESR linewidths for the compounds with different Sr content make it possible to estimate the values of the parameters in the expression for the linewidth: the maximal internal field  $H_{Gd}$  is about 200 Oe;  $\tau_\infty = 0.3 \cdot 10^{-12}$  sec and the corresponding activation energies  $E_a$  which are shown in Fig. 6. One of the key moments of the present study is the comparative Gd EPR analysis of the magnetic fluctuations for the different metalloxides, such as La<sub>2-x</sub>Sr<sub>x</sub>CuO<sub>4</sub> (LSCO) [23,24], La<sub>2-x</sub>Ba<sub>x</sub>CuO<sub>4</sub> (LBCO) [30], (La-Eu)<sub>2-x</sub>Sr<sub>x</sub>CuO<sub>4</sub> (LESCO) [25], (La-Nd)<sub>2-x</sub>Sr<sub>x</sub>CuO<sub>4</sub> (LNSCO) [8]. Note that for LBCO the measurements were restricted by the doping region in the vicinity of the well known  $T_c$  dip, whereas the last two series discussed in the previous part corresponded to the nonsuperconducting LTT phase. (Since the influence of the Nd magnetic moments for the LNSCO compound hinders the ESR measurements, the activation energy for this compound was estimated from the measurements of the nuclear spin relaxation on Cu and La nuclei [8]).

It is established [24] that for all LSCO based compounds the activation energy of magnetic fluctuations is enhanced near the 1/8 doping. This indicates the important role of the commensurability and gives evidence of the plane character of the inhomogeneous spin and charge distributions. The maximal

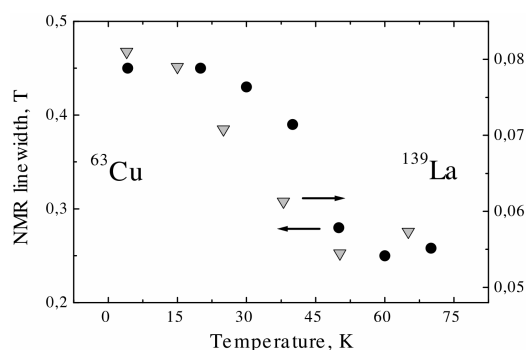


Fig. 7. The temperature dependence of the  $^{63}\text{Cu}$  and  $^{139}\text{La}$  NMR linewidths for the superconducting LSCO with  $x = 0.12$

magnetic fluctuations, which gradually freeze upon cooling. It allows us to estimate that the additional magnetic field at La nucleus is 0.015 T. If we consider that for the antiferromagnetic  $\text{La}_2\text{CuO}_4$  the copper moment of  $0.64 \mu_B$  induces the hyperfine field of 0.1 T at the La site [13], then the effective magnetic moment of copper in the superconducting LSCO is  $\sim 0.09 \mu_B$ .

#### IV. Conclusions

The Cu NQR analysis of the Eu doped  $\text{La}_{2-x}\text{Sr}_x\text{CuO}_4$  revealed that at 1.3 K the ground state of the LTT cuprates for moderate Sr content corresponds to the pinned stripe-phase and that the pinning is enhanced at the commensurability. Nonequivalent copper positions in the  $\text{CuO}_2$  planes were found. One of them with a magnetic moment of  $0.29 \mu_B$  is related to the AF correlated domains. From the behaviour of the NQR frequencies it follows that the effective charge of the domain walls separating these domains is almost independent on the Sr content  $x$ . The onset of the bulk superconductivity at larger  $x$  correlates with the dramatic transformation of the NQR spectra, indicating the depinning of the stripe phase and the crossover from the quasistatic to dynamical regime.

The combined ESR and NMR measurements of the LTO cuprates with the bulk superconductivity make it possible to conclude that the inherent feature of their superconducting state is the dynamical nanoscale phase separation. In the vicinity of hole doping  $x = 1/8$  this separation may be realized in a form of dynamic stripes – the corresponding enhancement of the spin-stiffness reveals the plane character of the spin (and charge) inhomogeneities. The characteristic fluctuation's frequencies are strongly inhomogeneous resulting in the coexistence of regions with quasistatic (frozen) and dynamical fluctuations.

According to our analysis the low temperature state of different lanthanum cuprates is strongly dependent on the spin-stiffness of the compound under study and it is possible to introduce the “critical” value of stiffness, which separates the compounds with the bulk superconducting phase from the nonsuperconducting ones.

#### V. Acknowledgements

The author dedicates this paper to the 70th birthday of Prof. B.I. Kochelaev – one of the pioneers of the ESR researches in the field of superconductivity.

This work was supported by RFBR through the Grant N 01-02-17533.

#### References

1. L.P. Gor'kov, A.V.Sokol, JETP Lett. 46 (1987) 420
2. D. Poilblanc and T.M. Rice, Phys. Rev., B 39, (1989) 9749; J. Zaanen and O. Gunnarson, Phys. Rev., B 40, (1989) 7391.
3. J.M. Tranquada *et al.*, Nature, 375, (1995) 561.
4. J.M. Tranquada, J. Phys. Chem. Solids, 59, (1998) 2150.
5. H.A. Mook *et al.*, Nature 395, (1998) 580.
6. H.P. Fong *et al.*, cond-mat/9902262.
7. A.W. Hunt *et al.*, Phys. Rev. Lett., 82, (1999) 4300.
8. G.B. Teitel'baum *et al.*, Phys.Rev.B 63 (2001) 020507(R).
9. G.B. Teitel'baum *et al.*, Phys.Rev.Lett., 84, (2000) 2949.
10. B. Büchner *et al.*, Physica, 185-189C, (1991) 903; Europhys. Lett., 21, (1993) 953.
11. T. Shimizu, J.Phys. Soc. Jpn., 62, (1993) 772.
12. R.L. Martin, Phys. Rev. Lett., 75, (1995) 744.
13. T. Tsuda *et al.*, J. Phys. Soc. Jpn., 57, (1988) 2908.
14. T. Imai *et al.*, Phys. Rev. Lett., 70, (1993) 1002.
15. G.M. Luke *et al.*, Hyp. Int., 105, (1997) 113.
16. M. Vojta, S. Sachdev, cond-mat/9906104.
17. B. Büchner *et al.*, Phys. Rev. Lett., 73, (1994) 1841.

18. K. Yoshimura *et al.*, *Hyp. Int.*, 79, (1993) 867; S. Oshugi *et al.*, *J. Phys. Soc. Jpn.*, 63, (1994) 2057.
19. P.C. Hammel *et al.*, *Phys. Rev. B* 57, (1998) R712.
20. J.M. Tranquada *et al.*, *Phys. Rev. Lett.*, 78 (1997) 338.
21. T. Suzuki *et al.*, *Phys. Rev. B* 57 (1998) R3229.
22. K. Yamada *et al.*, *Phys. Rev. B* 57 (1998) 6165.
23. P. Kuhns *et al.*, *Proc. of the Physical Phenomena in High Magnetic Fields-IV*. Santa Fe, NM, World Scientific (2002), 297.
24. G.B. Teitelbaum *et al.*, *JETP Lett* 72 (2003) 726.
25. V. Kataev *et al.*, *Phys. Rev. B* 58 (1998) R11876.
26. S.E. Barnes, *Adv. Phys.* 30 (1981) 801.
27. V. Kataev *et al.*, *JETP Lett*, 56 (1992) 385; *Phys. Rev. B* 48 (1993) 13042.
28. D.P. Arovas *et al.*, *Phys. Rev. Lett* 79 (1997) 2871.
29. B. Lake *et al.*, *Science* 291 (2001) 832.
30. B.Z. Rameev *et al.*, *Physica C* 246 (1995) 309.
31. S. Oshugi *et al.*, *J. Phys. Soc. Jpn.* 63 (1994) 2057.
32. T. Goto *et al.*, *J. Phys. Soc. Jpn.* 66 (1997) 2870.